

Chapter 4

Altitude Control of Helicopters with Unknown Dynamics

4.1 Introduction

The linearized models of Chap. 3 are useful not only for stability analysis, but also for control design, by gain scheduling the models at different operating points. This traditional technique has been successfully implemented in a wide variety of applications. However, it requires extensive modeling, which is costly and time-consuming, and the models are highly specific to a particular helicopter system. There is a need for controllers that can operate with minimal model information, handle nonlinearities over the entire flight regime, and are portable across different helicopter systems. In this chapter, we address this need by presenting a robust adaptive neural network (NN) control for helicopters.

Helicopter control design is challenging because helicopters are inherently unstable without closed loop control, differing from many classes of mechanical systems that are naturally passive or dissipative. Unrestrained helicopter motion is governed by underactuated configuration, i.e., the number of control inputs is less than the number of degrees of freedom to be stabilized, which makes it difficult to apply the conventional robotics approach for controlling Euler–Lagrange systems. In addition, helicopter dynamics are highly nonlinear and strongly coupled, such that disturbances along a single degree of freedom can easily propagate to the other degrees of freedom and lead to loss of performance or even destabilization.

Increasing effort has been made towards control design that guarantees stability for helicopter systems. Apart from the above-mentioned traditional linear control, many nonlinear techniques have been proposed, ranging from feedback linearization to model reference adaptive control and dynamic inversion. Dynamic sliding mode control was proposed for helicopter vertical regulation in [93]. Output tracking with nonhyperbolic and near nonhyperbolic internal dynamics in helicopter hover control was discussed in [19]. In [55], approximate input–output linearization was employed to obtain a dynamically linearizable helicopter system without zero dynamics, and output tracking was achieved. In [16], a high-bandwidth H_∞ loop shaping control was designed and tested for a robotic helicopter. Internal

model-based control was applied to the nonlinear motion control of a helicopter in [41]. In [104], model-based control was applied to the altitude and yaw angle tracking of a Lagrangian helicopter model.

Since helicopter control applications are characterized by unknown aerodynamical disturbances, they are generally difficult to model accurately. The presence of modeling errors, in the form of parametric and functional uncertainties, unmodeled dynamics, and disturbances from the environment, is a common problem. In this context, model-based control, such as the aforementioned schemes, tend to be susceptible to uncertainties and disturbances that cause performance degradation. How to handle model uncertainties and disturbances is one of the important issues in the control of helicopters.

Owing to the universal approximation capabilities, learning and adaptation, and parallel distributed structures of NNs, the feasibility of applying NNs to model unknown functions in dynamic systems has been demonstrated in several studies [23, 30, 32, 60, 61, 73]. As such, several flight control approaches using NNs have been proposed. Among of them, approximate dynamic inversion with augmented neural networks was proposed to handle unmodeled dynamics in [38, 53, 87], while neural dynamic programming was shown to be effective for tracking and trimming control of helicopters in [21]. During the adaptive trajectory control of an autonomous helicopter in [43] and [51], the method of pseudocontrol hedging (PCH) was used to protect the adaptation process from actuator limits and dynamics.

In this chapter, we propose an adaptive NN control for helicopters in vertical flight, which can be represented by single-input-single-output (SISO) models to yield useful results, because the coupling between longitudinal and lateral- directional equations in this flight regime is weak [10]. While the proposed controller handles vertical flight, other flight regimes can be handled by other control modules. Motivated by results in the NN control of nonlinear systems [30], we utilize Lyapunov-based techniques to design a robust adaptive NN control for helicopters with guaranteed stability. Although a nonaffine system can be rendered affine by adding an integrator to the control input, thus allowing many control methods for affine nonlinear system to be used, the disadvantage of this approach is that the dimension of the system is increased, and control efforts are not direct and immediate either [30]. Subsequently, effective control for the system may not be achieved. In this chapter, we focus on control design for the nonaffine system directly, without adding any integrators to the input.

Differing from the approaches in [38, 54], which were based on approximate dynamic inversion with augmented NNs, we utilize the Mean Value Theorem and the Implicit Function Theorem as mathematical tools to handle the nonaffine nonlinearities in the helicopter dynamics, based on the pioneering work of [31]. While the NNs in [38, 54] compensate for inaccuracy of the inversion model, those in our proposed scheme approximate the ideal feedback control law directly. In cases where reasonably accurate knowledge of the dynamic inversion model is available, the method of [38, 54] has been shown to provide an effective solution to the problem. However, the construction of the dynamic inversion for a nonaffine

system may not be an easy task in general. For such cases, our approach offers a feasible means of tackling the problem, since a priori knowledge of the inversion is not required.

4.2 Problem Formulation and Preliminaries

Consider the class of SISO helicopter systems described by the following differential equations nonaffine in the control:

$$\begin{aligned}\dot{x} &= f(x, u) \\ y &= h(x)\end{aligned}\tag{4.1}$$

where $x \in R^n$ are the states of the system; $u, y \in R$ denote the input and output respectively; and $f : R^n \times R \rightarrow R^n$ is an unknown function.

The control objective is output tracking of a desired reference trajectory such that the tracking error converges to a neighborhood of zero, i.e., $|y(t) - y_d(t)| \leq \delta$, where $\delta > 0$. At the same time, all closed loop signals are to be kept bounded. The reference trajectory $y_d(t)$ is generated by the following reference model:

$$\begin{aligned}\dot{\xi}_{di} &= \xi_{di+1}, \quad 1 \leq i \leq \rho - 1, \\ \dot{\xi}_{d\rho} &= f_d(\xi_d), \\ y_d &= \xi_{d1},\end{aligned}\tag{4.2}$$

where $\rho \geq 2$ is a constant index; $\xi_d = [\xi_{d1}, \xi_{d2}, \dots, \xi_{d\rho}]^T \in R^\rho$ are the states of the reference system; $y_d \in R$ is the system output; and $f_d : R^\rho \rightarrow R$ is a known function.

Assumption 4.1. The reference trajectory $y_d(t)$ and its ρ derivatives remain bounded, i.e., $\xi_d \in \Omega_d \subset R^\rho, \forall t \geq 0$, where ρ is the relative degree of (4.1).

Remark 4.1. The SISO representation considered in this chapter is valid for simple operations involving the regulation or tracking of single degree of freedom, such as altitude tracking or pitch regulation, among others.

Remark 4.2. System (4.1) is a general description of the nonlinear helicopter dynamics, for which the control input is not necessarily affine. This is a realistic representation for helicopters, due to the fact that the inputs are not torques or forces, which would yield an affine representation. Rather, the inputs are position variables implicit in aerodynamical forces or torques, resulting in a nonaffine form. Due to the lack of mathematical tools, the control design for such systems is very challenging. Note that control-affine nonlinear systems as well as linear systems are special cases of (4.1). As such, by designing a controller for (4.1), we cover the other systems as well.

Assumption 4.2. System (4.1) is input–output linearizable with strong relative degree $\rho < n$.

Define $\phi_j(x) = L_f^{j-1}h$ for $j = 1, \dots, \rho$, where $L_f h$ denotes the Lie derivative of the function $h(x)$ with respect to the vector field $f(x, u)$. Due to Assumption 4.2, it was shown in [39] that there exist other $n - \rho$ functions $\phi_{\rho+1}, \dots, \phi_n$ independent of u , such that the mapping $\Phi(x) = [\phi_1(x), \phi_2(x), \dots, \phi_n(x)]^T$ has a Jacobian matrix which is nonsingular for all $x \in \Omega_x$. Therefore, $\Phi(x)$ is a diffeomorphism on Ω_x . By setting $\xi = [\phi_1(x), \phi_2(x), \dots, \phi_\rho(x)]^T$ and $\eta = [\phi_{\rho+1}(x), \phi_{\rho+2}(x), \dots, \phi_n(x)]^T$, system (4.1) can be expressed in the normal form :

$$\begin{aligned}\dot{\eta} &= q(\eta, \xi) \\ \dot{\xi}_j &= \xi_{j+1}, \quad j = 1, \dots, \rho - 1 \\ \dot{\xi}_\rho &= b(\xi, \eta, u) \\ y &= \xi_1\end{aligned}\tag{4.3}$$

where $b(\xi, \eta, u) = L_f^{j-1}h$; $q(\xi, \eta) = [L_f \phi_{\rho+1}(x), L_f \phi_{\rho+2}(x), \dots, L_f \phi_n(x)]^T$; $x = \Phi^{-1}(\xi, \eta)$, for $(\xi, \eta, u) \in \bar{U} := \{(\xi, \eta, u) | (\xi, \eta) \in \Phi(\Omega_x); u \in \Omega_u\}$.

Assumption 4.3. The zero dynamics of system (4.3), given by $\dot{\eta} = q(0, \eta)$ are exponentially stable. In addition, the function $q(\xi, \eta)$ is Lipschitz in ξ , i.e.,

$$\|q(\xi, \eta) - q(0, \eta)\| \leq a_\xi \|\xi\| + a_q, \quad \forall (\xi, \eta) \in \Phi(\Omega_x)\tag{4.4}$$

Under Assumption 4.3, by the converse Lyapunov theorem, there exists a Lyapunov function $V_0(\eta)$ which satisfies the following inequalities:

$$\gamma_1 \|\eta\|^2 \leq V_0(\eta) \leq \gamma_2 \|\eta\|^2\tag{4.5}$$

$$\frac{\partial V_0}{\partial \eta} q(0, \eta) \leq -\lambda_a \|\eta\|^2\tag{4.6}$$

$$\left\| \frac{\partial V_0}{\partial \eta} \right\| \leq \lambda_b \|\eta\|\tag{4.7}$$

where $\gamma_1, \gamma_2, \lambda_a$, and λ_b are positive constants.

For ease of notation, define $g(x, u) := \frac{\partial b(\xi, \eta, u)}{\partial u}$. The following two assumptions specify some conditions on the unknown function $g(x, u)$.

Assumption 4.4. There exist smooth functions $\bar{g}(\xi, \eta)$ and a positive constant $\underline{g} > 0$, such that $\bar{g}(\xi, \eta) \geq |g(\xi, \eta, u)| \geq \underline{g} > 0$ holds for all $(\xi, \eta, u) \in \bar{U}$. Without loss of generality, it is further assumed that the sign of $g(\xi, \eta, u)$ is positive for all $(\xi, \eta, u) \in \bar{U}$.

Assumption 4.5. There exist a positive function $g_0(\xi, \eta)$ such that $|\dot{g}(\xi, \eta, u)| \leq 2g(\xi, \eta, u)g_0(\xi, \eta)$, $\forall (\xi, \eta, u) \in \bar{U}$.

Remark 4.3. Assumption 4.4 implies that partial derivative $g(\xi, \eta, u)$ has a fixed sign. In addition, it means that the Taylor series linearization is controllable so one could always linearize and design a linear controller, if possible. This assumption is standard and necessary as otherwise, the system is not controllable.

Based on Assumption 4.4, the following lemma is given to assert the existence of an implicit desired function, which will be used in the design of the NN controller.

Lemma 4.4 (Implicit Function Theorem). [33] *For a continuously differentiable function $b(\xi, \eta, u) : R^n \times R \rightarrow R$ satisfying Assumption 4.4, there exists a continuous (smooth) function $u^* = u(\xi, \eta)$ such that $b(\xi, \eta, u^*) = 0$.*

Lemma 4.5 (Mean Value Theorem). [1] *Assume that $f(x, y) : R^n \times R \rightarrow R$ has a derivative (finite or infinite) at each point of an open set $R^n \times (a, b)$, and assume also that it is continuous at both endpoints $y = a$ and $y = b$. Then there is a point $\xi \in (a, b)$ such that $f(x, b) - f(x, a) = f'(x, \xi)(b - a)$.*

Remark 4.6. It should be emphasized that the Mean Value Theorem gives an equality condition and is different from Taylor series expansion, which only gives an approximation when the higher order terms are truncated.

Remark 4.7. The combination of the Implicit Function Theorem, the Mean Value Theorem, and NNs is instrumental to solving the control problem for generalized nonaffine helicopter systems described by (4.1). While the Implicit Function Theorem asserts the existence of a desired control, it does not provide any means of constructing it. NNs are thus employed for this purpose. On the other hand, the Mean Value Theorem expresses the nonaffine function into a form where the actual and desired inputs are linearly matched, facilitating the design of adaptive NN control via certainty equivalence and Lyapunov-based techniques. These will be elaborated in detail in the subsequent developments.

Lastly, we present the following definition and Lemma, which are important for stability and performance analysis.

Definition 4.8. The solution of (4.1) is Semi-Globally Uniformly Ultimately Bounded (SGUUB) if, for any compact set Ω_0 , there exists an $S > 0$ and $T(S, X(t_0))$ such that $\|X(t)\| \leq S$ for all $X(t_0) \in \Omega_0$ and $t \geq t_0 + T$.

Lemma 4.9. [34] *Suppose that there exists a C^1 continuous and positive definite Lyapunov function $V(x)$ satisfying*

$$\gamma_1(\|x\|) \leq V(x) \leq \gamma_2(\|x\|), \quad (4.8)$$

such that

$$\dot{V}(x) \leq -c_1 V(x) + c_2, \quad (4.9)$$

where $\gamma_1, \gamma_2 : R^n \rightarrow R$ are class K_∞ functions and c_1, c_2 are positive constants, then the solution $x(t)$ is SGUUB.

4.3 Function Approximation with Neural Networks

Due to the existence of model uncertainties in practice, we introduce a NN here to approximate and compensate for them using the good function approximation capability of NN. In particular, two types of NN will be discussed, i.e., the radial basis function neural network (RBFNN), which is linearly parameterized; and the multilayer neural network (MNN), which is nonlinearly parameterized.

4.3.1 Function Approximation with RBFNN

The RBFNN can be used to approximate the continuous function $f(Z) : R^m \rightarrow R$ as follows:

$$f(Z) = W^T S(Z) + \varepsilon(Z) \quad (4.10)$$

where the input vector $Z \in \Omega_Z \subset R^m$; weight vector $W = [w_1, w_2, \dots, w_l]^T \in R^l$, the NNs node number $l > 1$; $S(Z) = [s_1(Z), \dots, s_l(Z)]^T$, with $s_i(Z)$ being chosen as the commonly used Gaussian functions, which have the form:

$$s_i(Z) = \exp \left[\frac{-(Z - \mu_i)^T (Z - \mu_i)}{\eta_i^2} \right], \quad i = 1, 2, \dots, l$$

where $\mu_i = [\mu_{i1}, \mu_{i2}, \dots, \mu_{im}]^T$ is the center of the receptive field and η_i is the width of the Gaussian function; and $\varepsilon(Z)$ is the approximation error which is bounded over the compact set Ω_Z , i.e., $|\varepsilon(Z)| \leq \bar{\varepsilon}$, $\forall Z \in \Omega_Z$ where $\bar{\varepsilon} > 0$ is an unknown constant.

It has been proven that RBFNN (4.10) can approximate any continuous function $f(Z)$ over a compact set $\Omega_Z \subset R_m$ to arbitrarily any degree of accuracy as

$$f(Z) = W^{*T} S(Z) + \varepsilon^*(Z), \quad \forall Z \in \Omega_Z \subset R^m \quad (4.11)$$

where W^* is ideal constant weights, and $\varepsilon^*(Z)$ is the approximation error for the special case where $W = W^*$.

Assumption 4.6. On the compact set Ω_Z , the ideal NN weights W^* is bounded by

$$\|W^*\| \leq w_m \quad (4.12)$$

The ideal weight vector W^* is defined as the value of W that minimizes $|\varepsilon(Z)|$ for all $Z \in \Omega_Z \subset R^m$:

$$W^* = \arg \min_W \{ \sup_{Z \in \Omega_Z} |f(Z) - W^T S(Z)| \}$$

In general, the ideal weights W^* are unknown and need to be estimated in control design. Let \hat{W} be the estimates of W^* , and the weight estimation errors $\tilde{W} = \hat{W} - W^*$.

4.3.2 Function Approximation with MNN

The other popular type of NN, nonlinearly parameterized MNN, is used to approximate the continuous function $f(Z) : R^m \rightarrow R$ as follows:

$$f(Z) = W^T S(V^T Z) + \varepsilon(Z)$$

where the vector $Z = [z_1, z_2, \dots, z_m, 1]^T \in \Omega_Z \subset R^{m+1}$ are the input variables to the NNs; $S(\cdot) \in R^l$ is a vector of known continuous basis functions, with l denoting the number of neural nodes; $W \in R^l$ and $V \in R^{(m+1) \times l}$ are adaptable weights; and $\varepsilon(Z)$ is the approximation error which is bounded over the compact set Ω_Z , i.e., $|\varepsilon(Z)| \leq \bar{\varepsilon}$, $\forall Z \in \Omega_Z$ where $\bar{\varepsilon} > 0$ is an unknown constant.

According to the universal approximation property [27], MNNs can smoothly approximate any continuous function $f(Z)$ over a compact set $\Omega_Z \subset R^{m+1}$ to arbitrarily any degree of accuracy as that

$$f(Z) = W^{*T} S(V^{*T} Z) + \varepsilon^*(Z), \quad \forall Z \in \Omega_Z \subset R^{m+1}$$

where W^* and V^* are the ideal constant weights, and $\varepsilon^*(Z)$ is the approximation error for the special case where $W = W^*$ and $V = V^*$. The ideal weights W^* and V^* are defined as the values of W and V that minimize $|\varepsilon(Z)|$ for all $Z \in \Omega_Z \subset R^{m+1}$, i.e.,

$$(W^*, V^*) := \arg \min_{(W, V)} \{ \sup_{Z \in \Omega_Z} |f(Z) - W^T S(V^T Z)| \}$$

Assumption 4.7. On the compact set Ω_Z , the ideal NN weights W^* , V^* are bounded by

$$\|W^*\| \leq w_m, \quad \|V^*\|_F \leq v_m$$

In general, the ideal weights W^* and V^* are unknown and need to be estimated in control design. Let \hat{W} and \hat{V} be the estimates of W^* and V^* , respectively, and the weight estimation errors $\tilde{W} = \hat{W} - W^*$ and $\tilde{V} = \hat{V} - V^*$.

Lemma 4.10. [30] Using $f_{mnn} = \hat{W}^T S(\hat{V}^T Z)$ to approximate the ideal function $f(Z)$, its approximation error can be expressed as

$$\hat{W}^T S(\hat{V}^T Z) - W^{*T} S(V^{*T} Z) = \tilde{W}^T (\hat{S} - \hat{S}' \hat{V}^T Z) + \hat{W}^T \hat{S}' \tilde{V}^T Z + d_u$$

where $\hat{S} = S(\hat{V}^T Z)$, $\hat{S}' = \text{diag} \{\hat{s}'_1, \hat{s}'_2, \dots, \hat{s}'_l\}$ with

$$\hat{s}'_i = s'(\hat{v}_i^T Z) = \left. \frac{d[s(z_a)]}{dz_a} \right|_{z_a = \hat{v}_i^T Z}$$

and the residual term d_u is bounded by

$$|d_u| \leq \|V^*\|_F \|Z \hat{W}^T \hat{S}'\|_F + \|W^*\| \|\hat{S}' \hat{V}^T Z\| + |W^*|_1$$

Throughout this chapter, we employ sigmoidal functions as basis functions for the MNN, which are defined by

$$s_i(z_a) = \frac{1}{1 + e^{-\mu z_a}}, \quad i = 1, 2, \dots, l \quad (4.13)$$

where $\mu > 0$ is a design constant.

4.4 Adaptive NN Control Design

We employ backstepping for the ξ subsystem, and then make use of the exponential stability of the zero dynamics to show that the overall closed-loop system is stable and that output tracking is achieved. The control design is performed first for the full state case and subsequently for the output feedback case with high gain observers.

4.4.1 Full State Feedback Control

Step 1: Let $z_1(t) = \xi_1(t) - y_d(t)$ and $z_2(t) = \xi_2(t) - \alpha_1(t)$, where $\alpha_1(t)$ is a virtual control function to be determined. Define quadratic function $V_1 = \frac{1}{2} z_1^2$. Choosing the virtual control α_1 as

$$\alpha_1 = -k_1 z_1 + \dot{y}_d, \quad (4.14)$$

we can show that

$$\dot{V}_1 = -k_1 z_1^2 + z_1 z_2, \quad (4.15)$$

where the term $z_1 z_2$ will be canceled in the subsequent step.

Step i (i = 2, ..., ρ - 1): Let $z_i(t) = \xi_i(t) - \alpha_{i-1}(t)$, where $\bar{\xi}_i := [\xi_1, \dots, \xi_i]^T$ and $\alpha_i(t)$ is a virtual control function to be determined. Define quadratic function $V_i = V_{i-1} + \frac{1}{2}z_i^2$. Choose the virtual control α_i as

$$\alpha_i = -k_i z_i - z_{i-1} + \dot{\alpha}_{i-1}, \quad (4.16)$$

where the derivative can be written as

$$\dot{\alpha}_{i-1} = \frac{\partial \alpha_{i-1}}{\partial \bar{\xi}} \dot{\bar{\xi}} + \sum_{k=0}^{i-1} \frac{\partial \alpha_{i-1}}{\partial y_d^{(k)}} y_d^{(k+1)}. \quad (4.17)$$

It can be shown that

$$\dot{V}_i = -\sum_{j=1}^i k_j z_j^2 + z_i z_{i+1}, \quad (4.18)$$

where the term $z_i z_{i+1}$ will be canceled in the subsequent step.

Step ρ: This is the final step where the actual control law u will be designed.

From Assumption 2, we know that $g(\xi, \eta, u) \geq d > 0$ for all $(\xi, \eta, u) \in R^{n+1}$. Define v as

$$v = -\dot{\alpha}_{\rho-1} + g_0(\xi, \eta)z_\rho, \quad (4.19)$$

where $k_n > 0$ is a constant. It is clear that v is a function of $\xi, \eta, y_d, y_d^{(1)}, \dots, y_d^{(\rho)}$. Considering the fact that $\frac{\partial v}{\partial u} = 0$, the following inequality holds

$$\frac{\partial [b(\xi, \eta, u) + v]}{\partial u} \geq d > 0. \quad (4.20)$$

According to Lemma 1, for every value of ξ, η and v , there exists a smooth ideal control input $u \in R$ such that

$$b(\xi, \eta, u^*) + v = 0, \quad (4.21)$$

Using the Mean Value Theorem in Lemma 4.5, there exists $(0 < \lambda < 1)$ such that

$$b(\xi, \eta, u) = b(\xi, \eta, u^*) + g_\lambda(u - u^*), \quad (4.22)$$

where $g_\lambda := g(\xi, \eta, u_\lambda)$. Combining (4.19)–(4.22) yields

$$\dot{z}_\rho = -g_0(\xi, \eta)z_\rho + g_\lambda(u - u^*). \quad (4.23)$$

We employ a robust MNN controller of the form:

$$u = u_{nn} + u_b, \quad (4.24)$$

where

$$u_{nn} = \hat{W}^T S(\hat{V}^T Z), \quad (4.25)$$

$$u_b = -k_\rho z_\rho - z_{\rho-1} - k_b \left(\|Z \hat{W}^T \hat{S}'\|_F^2 + \|\hat{S}' \hat{V}^T Z\|^2 \right) z_\rho. \quad (4.26)$$

The component u_{nn} is an MNN that approximates $u^*(\xi, \eta)$, which can be expressed as

$$u^* = W^{*T} S(V^{*T} Z) + \varepsilon, \quad (4.27)$$

where $Z = [\xi, \eta, z_\rho, \dot{\alpha}_{\rho-1}]^T \in \Omega \subset R^{n+2}$; W^* denotes the vector of ideal constant weights, and $|\varepsilon| \leq \bar{\varepsilon}$ is the approximation error with constant $\bar{\varepsilon} > 0$. As detailed in [30], the component u_b ensures robustness to the approximation error of the MNN.

Consider the Lyapunov function candidate

$$V_\rho = V_{\rho-1} + \frac{1}{2g_\lambda} z_\rho^2 + \frac{1}{2} \tilde{W}^T \Gamma_W^{-1} \tilde{W} + \frac{1}{2} \text{tr} \{ \tilde{V}^T \Gamma_V^{-1} \tilde{V} \}, \quad (4.28)$$

where $\tilde{W} := \hat{W} - W^*$ and $\tilde{V} := \hat{V} - V^*$. The derivative of V_ρ is

$$\begin{aligned} \dot{V}_\rho &= -\sum_{j=1}^{\rho-1} k_j z_j^2 + z_{\rho-1} z_\rho + \frac{z_\rho \dot{z}_\rho}{g_\lambda} - \frac{\dot{g}_\lambda z_\rho^2}{2g_\lambda^2} + \tilde{W}^T \Gamma_W^{-1} \dot{\tilde{W}} + \text{tr} \{ \tilde{V}^T \Gamma_V^{-1} \dot{\tilde{V}} \} \\ &= -\sum_{j=1}^{\rho-1} k_j z_j^2 + z_{\rho-1} z_\rho - \frac{g_0}{g_\lambda} z_\rho^2 - \frac{\dot{g}_\lambda}{2g_\lambda^2} z_\rho^2 + z_\rho(u - u^* - \varepsilon) + \tilde{W}^T \Gamma_W^{-1} \dot{\tilde{W}} \\ &\quad + \text{tr} \{ \tilde{V}^T \Gamma_V^{-1} \dot{\tilde{V}} \} \\ &= -\sum_{j=1}^{\rho-1} k_j z_j^2 + z_{\rho-1} z_\rho - \left(g_0 + \frac{\dot{g}_\lambda}{2g_\lambda} \right) \frac{z_\rho^2}{g_\lambda} + \tilde{W}^T \left[(\hat{S} - \hat{S}' \hat{V}^T Z) z_\rho \right. \\ &\quad \left. + \Gamma_W^{-1} \dot{\tilde{W}} \right] + \text{tr} \left\{ \tilde{V}^T [Z \hat{W}^T \hat{S}' z_\rho] + \Gamma_V^{-1} \dot{\tilde{V}} \right\} + z_\rho(d_u + u_b) \\ &\quad - z_\rho \varepsilon \end{aligned} \quad (4.29)$$

Consider the following adaptation laws

$$\dot{\hat{W}} = -\Gamma_W \left[(\hat{S} - \hat{S}' \hat{V}^T Z) z_\rho + \sigma_W \hat{W} \right] \quad (4.30)$$

$$\dot{\hat{V}} = -\Gamma_V \left[Z \hat{W}^T \hat{S}' z_\rho + \sigma_V \hat{V} \right] \quad (4.31)$$

where $\Gamma_W = \Gamma_W^T > 0$, $\Gamma_V = \Gamma_V^T > 0$, $\sigma_W > 0$ and $\sigma_V > 0$ are constant design parameters. Then, substituting (4.26), (4.30), and (4.31) into (4.29) yields

$$\begin{aligned} \dot{V}_\rho &= -\sum_{j=1}^{\rho-1} k_j z_j^2 + z_{\rho-1} z_\rho - \left(g_0 + \frac{\dot{g}_\lambda}{2g_\lambda} \right) \frac{z_\rho^2}{g_\lambda} - \sigma_W \tilde{W}^T \hat{W} - \sigma_V \text{tr}\{\tilde{V}^T \hat{V}\} \\ &\quad - z_\rho \varepsilon + z_\rho (d_u + u_b) \\ &\leq -\sum_{j=1}^{\rho-1} k_j z_j^2 - \left(g_\lambda k_\rho + g_0 + \frac{\dot{g}_\lambda}{2g_\lambda} \right) \frac{z_\rho^2}{g_\lambda} - \sigma_W \tilde{W}^T \hat{W} - \sigma_V \text{tr}\{\tilde{V}^T \hat{V}\} \\ &\quad - z_\rho \varepsilon + |z_\rho| \left(\|W^* \| \|\hat{S}' \hat{V}^T Z\| + \|V^* \|_F \|Z \hat{W}^T \hat{S}' \|_F + \|W^* \| \right) \\ &\quad - k_b \left(\|S' \hat{V}^T Z\|^2 + \|Z \hat{W}^T S'\|_F^2 \right) z_\rho^2 \\ &\leq -\sum_{j=1}^{\rho-1} k_j z_j^2 - \left(g_\lambda (k_\rho - 1) + g_0 + \frac{\dot{g}_\lambda}{2g_\lambda} \right) \frac{z_\rho^2}{g_\lambda} - \sigma_W \tilde{W}^T \hat{W} - \sigma_V \text{tr}\{\tilde{V}^T \hat{V}\} \\ &\quad + \|W^* \|^2 + \frac{1}{2} \|V^* \|_F^2 - \left(k_b - \frac{1}{2} \right) \left(\|\hat{S}' \hat{V}^T Z\|^2 + \|Z \hat{W}^T \hat{S}' \|_F^2 \right) z_\rho^2 + \frac{1}{2} \varepsilon^2 \end{aligned} \quad (4.32)$$

By completion of squares, the following inequalities hold

$$-\sigma_W \tilde{W}^T \hat{W} \leq \frac{\sigma_W}{2} (-\|\tilde{W}\|^2 + \|W^*\|^2) \quad (4.33)$$

$$-\sigma_V \text{tr}\{\tilde{V}^T \hat{V}\} \leq \frac{\sigma_V}{2} (-\|\tilde{V}\|_F^2 + \|V^*\|_F^2) \quad (4.34)$$

Substituting (4.33) and (4.34) into (4.32) yields the following

$$\begin{aligned} \dot{V}_\rho &\leq -\sum_{j=1}^{\rho-1} k_j z_j^2 - \left(g_\lambda (k_\rho - 1) + g_0 + \frac{\dot{g}_\lambda}{2g_\lambda} \right) \frac{z_\rho^2}{g_\lambda} - \left(k_b - \frac{1}{2} \right) \left(\|\hat{S}' \hat{V}^T Z\|^2 \right. \\ &\quad \left. + \|Z \hat{W}^T \hat{S}' \|_F^2 \right) z_\rho^2 - \frac{\sigma_W}{2} \|\tilde{W}\|^2 - \frac{\sigma_V}{2} \|\tilde{V}\|_F^2 + \frac{1}{2} \varepsilon^2 + \frac{\sigma_W + 2}{2} \|W^*\|^2 \\ &\quad + \frac{\sigma_V + 1}{2} \|V^*\|_F^2 \end{aligned} \quad (4.35)$$

From Assumption 4.5, we know that $\left(g_0 + \frac{\dot{g}\lambda}{2g\lambda}\right) \geq 0$. Hence, by choosing the control parameters k_ρ and k_b as follows

$$k_\rho > 1, \quad k_b > \frac{1}{2} \quad (4.36)$$

the second and third right-hand-side (RHS) terms of (4.35) are strictly negative, thus leading to the following simplification

$$\begin{aligned} \dot{V}_\rho &\leq -\sum_{j=1}^{\rho-1} k_j z_j^2 - (k_\rho - 1) z_\rho^2 - \frac{\sigma_W}{2} \|\tilde{W}\|^2 - \frac{\sigma_V}{2} \|\tilde{V}\|_F^2 \\ &\quad + \frac{1}{2} \bar{\varepsilon}^2 + \frac{\sigma_W + 2}{2} \|W^*\|^2 + \frac{\sigma_V + 1}{2} \|V^*\|_F^2 \\ &\leq -c_1 V_\rho + c_2 \end{aligned} \quad (4.37)$$

where

$$c_1 = \min \left\{ 2k_1, 2k_2, \dots, 2k_{\rho-1}, 2\underline{g}(k_\rho - 1), \frac{\sigma_W}{\lambda_{\max}(\Gamma_W^{-1})}, \frac{\sigma_V}{\lambda_{\max}(\Gamma_V^{-1})} \right\} \quad (4.38)$$

$$c_2 = \frac{1}{2} \bar{\varepsilon}^2 + \frac{\sigma_W + 2}{2} \|W^*\|^2 + \frac{\sigma_V + 1}{2} \|V^*\|_F^2 \quad (4.39)$$

The following lemma is useful for stability analysis of the internal dynamics.

Lemma 4.11. *Given that Assumptions 4.1 and 4.3 are satisfied, there exist positive constants a_1 , a_2 and T_0 such that the trajectories $\eta(t)$ of the internal dynamics satisfy*

$$\|\eta(t)\| \leq a_1(\|z(t)\| + \|\xi_d(t)\|) + a_2 \quad \forall t > T_0. \quad (4.40)$$

Proof. The proof is very similar to that given in [35]. For completeness, it is shown here. According to Assumption 4.3, there exists a Lyapunov function $V_0(\eta)$. Differentiating $V_0(\eta)$ along (4.3) yields

$$\begin{aligned} \dot{V}_0(\eta) &= \frac{\partial V_0}{\partial \eta} q(\xi, \eta) \\ &= \frac{\partial V_0}{\partial \eta} q(0, \eta) + \frac{\partial V_0}{\partial \eta} (q(\xi, \eta) - q(0, \eta)). \end{aligned} \quad (4.41)$$

Noting (4.4)–(4.7), (4.41) can be written as

$$\dot{V}_0 \leq -\lambda_a \|\eta\|^2 + \lambda_b a_\xi \|\eta\| \|\xi\| + \lambda_b a_q \|\eta\|. \quad (4.42)$$

From the fact that $\|\xi\| \leq \|z\| + \|\xi_d\|$, where $\xi_d := [y_d, \alpha_1, \alpha_2, \dots, \alpha_{\rho-1}]^T$, we obtain the following:

$$\dot{V}_0(\eta) \leq \lambda_a \|\eta\|^2 + \lambda_b \|\eta\| (a_\xi \|\xi_d\| + a_q + a_\xi \|z\|). \quad (4.43)$$

Therefore, $\dot{V}_0(\eta) \leq 0$ whenever

$$\|\eta\| \geq \frac{\lambda_b}{\lambda_a} (a_\xi \|\xi_d\| + a_q + a_\xi \|z\|). \quad (4.44)$$

By letting

$$a_1 = \frac{\lambda_b a_\xi}{\lambda_a}, \quad a_2 = \frac{\lambda_b a_q}{\lambda_a}, \quad (4.45)$$

we conclude that there exist T_0 such that (4.40) holds. \square

We summarize our results for the full-state feedback case in the following theorem.

Theorem 4.12. *Consider the SISO helicopter dynamics (4.1) satisfying Assumptions 4.1–4.5, with control law (4.24) and adaptation laws (4.30)–(4.31). For initial conditions $\xi(0)$, $\eta(0)$, $\tilde{W}(0)$, $\tilde{V}(0)$ belonging to any compact set Ω_0 , all closed loop signals are SGUUB, and the tracking error $z_1 = y - y_d$ converges to the compact set*

$$\Omega_{z_1} := \left\{ z_1 \in R \mid \|z_1\| \leq \sqrt{\frac{2c_2}{c_1}} \right\}, \quad (4.46)$$

where c_1 and c_2 are constants defined in (4.38) and (4.39), respectively.

Proof. According to Lemma 1.1–1.2 in [34], we know from (4.37) that z , \tilde{W} and \tilde{V} are bounded within the compact sets for all $t > 0$:

$$\Omega_z = \left\{ z \in R^\rho \mid \|z\| \leq \sqrt{2 \left(V_\rho(0) + \frac{c_2}{c_1} \right)} \right\}, \quad (4.47)$$

$$\Omega_W = \left\{ \tilde{W} \in R^l \mid \|\tilde{W}\| \leq \sqrt{\frac{2 \left(V_\rho(0) + \frac{c_2}{c_1} \right)}{\lambda_{\min}(\Gamma_W^{-1})}} \right\}, \quad (4.48)$$

$$\Omega_V = \left\{ \tilde{V} \in R^{(m+1) \times l} \left| \|\tilde{V}\|_F \leq \sqrt{\frac{2 \left(V_\rho(0) + \frac{c_2}{c_1} \right)}{\lambda_{\min}(\Gamma_V^{-1})}} \right. \right\}. \quad (4.49)$$

Since W^* and V^* are bounded, it is obvious that \hat{W} and \hat{V} are also bounded.

From (4.14), (4.16), and the fact that z , y_d , $y_d^{(1)}$, ..., $y_d^{(\rho)}$ are bounded, we know that the virtual controls α_i , $i = 1, 2, \dots, \rho$ are bounded. Hence, there exists a constant $a_3 > 0$ such that $\|\xi_d\| \leq a_3$.

From Lemma 4.11, it can be seen that η is bounded if both z and ξ_d are bounded. As a result, we can conclude that the states of the internal dynamics will converge to the compact set

$$\Omega_\eta := \left\{ \eta \in R^{n-\rho} \left| \|\eta\| \leq a_1 \left(\sqrt{\frac{2c_2}{c_1}} + a_3 \right) + a_2 \right. \right\}, \quad (4.50)$$

where a_1 and a_2 are defined in (4.45). Since the control signal $u(t)$ is a function of the weights $\hat{W}(t)$, $\hat{V}(t)$ and the states $\xi(t)$, $\eta(t)$, we know that it is also bounded. Therefore, we have shown that all the closed loop signals are SGUUB.

To show that the tracking error $z_1 = y - y_d$ converges to the compact set Ω_{z_1} , we multiply (4.37) by $e^{-c_1 t}$ and integrate over $[0, t]$ to obtain that

$$|z(t)| \leq \sqrt{2 \left(V_\rho(0) + \frac{c_2}{c_1} \right) e^{-c_1 t} + 2 \frac{c_2}{c_1}}, \quad (4.51)$$

from which it is easy to see that $|z_1(t)| \leq \sqrt{\frac{2c_2}{c_1}}$ as $t \rightarrow \infty$. \square

Remark 4.13. From Theorem 4.12, we know that the size of the steady state compact set Ω_{z_1} , to which the tracking error converges, is governed by the constants c_1 and c_2 , which in turn depend on the control and NN parameters. It follows that by appropriate tuning of the parameters, the guaranteed upper bound for the steady state tracking error can be reduced. For instance, increasing the control gains k_1, \dots, k_ρ increases c_1 accordingly, and leads to a reduction in the size of Ω_{z_1} .

Remark 4.14. Although the theoretical results in this chapter are obtained under Assumption 4.4 that $g_\lambda(\cdot) > 0$, there is no loss of generality. For the case of $g_\lambda(\cdot) < 0$, the Lyapunov function candidate (4.28) can be changed to

$$V_\rho = V_{\rho-1} - \frac{1}{2g_\lambda} z_\rho^2 + \frac{1}{2} \tilde{W}^T \Gamma_W^{-1} \tilde{W} + \frac{1}{2} \text{tr} \{ \tilde{V}^T \Gamma_V^{-1} \tilde{V} \}, \quad (4.52)$$

for which a correspondingly stable controller can be constructed as $u = -u_{nn} - u_b$, where u_{nn} and u_b are defined in (4.25) and (4.26) respectively.

4.4.2 Output Feedback Control

In the previous section, we have considered the case where full state measurement is possible, that is, η and ξ are all available. In this section, we tackle the output feedback problem, where only η and ξ_1 are available, by utilizing high gain observers.

Lemma 4.15. [7, 35] *Consider the following linear system:*

$$\begin{aligned}\epsilon \dot{\pi}_i &= \pi_{i+1}, \quad i = 1, 2, \dots, \rho - 1, \\ \epsilon \dot{\pi}_\rho &= -\gamma_1 \pi_\rho - \gamma_2 \pi_{\rho-1} - \dots - \gamma_{\rho-1} \pi_2 - \pi_1 + \xi_1(t),\end{aligned}\quad (4.53)$$

where ϵ is a small positive constant and the parameters γ_1 to $\gamma_{\rho-1}$ are chosen such that the polynomial $s^\rho + \gamma_1 s^{\rho-1} + \dots + \gamma_{\rho-1} s + 1$ is Hurwitz. Suppose the states ξ belong to a compact set, so that $|\xi_k| < Y_k$, then the following property holds:

$$\tilde{\xi}_k := \frac{\pi_k}{\epsilon^{k-1}} - \xi_k = -\epsilon \zeta^{(k)}, \quad k = 1, 2, \dots, \rho, \quad (4.54)$$

where $\zeta := \pi_\rho + \gamma_1 \pi_{\rho-1} + \dots + \gamma_{\rho-1} \pi_1$ and $\zeta^{(k)}$ denotes the k -th derivative of ζ . Furthermore, there exist positive constants h_k and t^* such that $|\tilde{\xi}_k| \leq \epsilon h_k$ is satisfied for $t > t^*$.

Proof. Differentiating the last equation of (4.53) with respect to time and substituting into $\frac{\pi_2}{\epsilon} - \dot{\chi}$ yields

$$\frac{\pi_2}{\epsilon} - \dot{\chi} = \frac{\pi_2}{\epsilon} - \epsilon \ddot{\pi}_n - \gamma_1 \dot{\pi}_n - \gamma_2 \dot{\pi}_{n-1} - \dots - \gamma_{n-1} \dot{\pi}_2 - \dot{\pi}$$

Noting from (4.53) that $\dot{\pi}_i = \epsilon \ddot{\pi}_{i-1}$ for $i = 2, 3, \dots, n$ leads to

$$\begin{aligned}\frac{\pi_2}{\epsilon} - \dot{\chi} &= -\epsilon(\ddot{\pi}_n + \gamma_1 \ddot{\pi}_{n-1} + \gamma_2 \ddot{\pi}_{n-2} + \dots + \gamma_{n-1} \ddot{\pi}_1) \\ &= -\epsilon \ddot{\zeta}\end{aligned}$$

By repeatedly differentiating the above and utilizing (4.53), we arrive at (4.54).

To show that $|\tilde{y}(t)| \leq \epsilon h_k$ for $t > t^*$, we first note that the derivatives of the vector $[\pi_1 \ \pi_2 \ \dots \ \pi_\rho]^T$ can be computed as follows

$$\begin{aligned}\pi^{(j)}(t) &= \frac{1}{\epsilon^j} A^j e^{\frac{At}{\epsilon}} [\pi(0) + A^{-1} b y(0) + \epsilon A^{-2} b y^{(1)}(0) \\ &\quad + \dots + \epsilon^{j-1} A^{-j} b y^{(j-1)}(0)] \\ &\quad + \frac{1}{\epsilon} e^{\frac{At}{\epsilon}} \int_0^t e^{-\frac{A\tau}{\epsilon}} b y^{(j)}(\tau) d\tau\end{aligned}\quad (4.55)$$

for $j = 1, 2, \dots, \rho$, where

$$A = \begin{bmatrix} 0 & 1 & 0 & \cdots & 0 \\ 0 & 0 & 1 & \cdots & 0 \\ \cdots & \cdots & \cdots & \cdots & \cdots \\ 0 & 0 & 0 & \cdots & 1 \\ -1 & \gamma_1 & \gamma_2 & \cdots & \gamma_{\rho-1} \end{bmatrix}, \quad b = \begin{bmatrix} 0 \\ 0 \\ \vdots \\ 0 \\ 1 \end{bmatrix} \quad (4.56)$$

Since ξ belongs to a compact set, and u is bounded, we know that $|y^{(j)}| \leq Y_j$. Therefore, there exists a constant $t^* > 0$ such that for $t > t^*$, $|\pi^{(j)}(t)| \leq D_j$, where D_j is a positive constant independent of ϵ . This leads to $|\zeta^{(j)}| \leq h_j := BD_j$, where B is the norm of $[1 \ \gamma_1 \ \gamma_2 \ \dots \ \gamma_{\rho-1}]^T$. \square

Remark 4.16. Note that $\frac{\pi_k}{\epsilon^{k-1}}$ converges to a neighborhood of ξ_k , provided that y and its derivatives up to the ρ -th order are bounded. Hence, $\frac{\pi_{k+1}}{\epsilon^k}$ is a suitable observer to estimate the k th order output derivative.

To prevent peaking [52], saturation functions are employed on the observer signals whenever they are outside the domain of interest:

$$\pi_i^s = \bar{\pi}_i \operatorname{sat}\left(\frac{\pi_i}{\bar{\pi}_i}\right), \quad \bar{\pi}_i \geq \max_{(z, \hat{W}, \hat{V}) \in \Omega} (\pi_i), \quad \operatorname{sat}(a) = \begin{cases} -1 & \text{for } a < -1 \\ a & \text{for } |a| \leq 1 \\ 1 & \text{for } a > 1 \end{cases} \quad (4.57)$$

for $i = 1, 2, \dots, \rho$, where $\tilde{\xi} = [\tilde{\xi}_1, \dots, \tilde{\xi}_\rho]^T$, and the compact set $\Omega := \Omega_z \times \Omega_W \times \Omega_V$, where Ω_z , Ω_W , and Ω_V are defined in (4.47), (4.48), and (4.49) respectively, denotes the domain of interest.

Now, we revisit the control law (4.24)–(4.26) and adaptation laws (4.30)–(4.31) for the full-state feedback case. Via the certainty equivalence approach, we modify them by replacing the unavailable quantities z_i and Z with their estimates, $\hat{z}_i := \frac{\pi_i^s}{\epsilon^{i-1}} - \hat{\alpha}_{i-1}$ and $\hat{Z} := [\hat{\xi}_1, \frac{\pi_2^s}{\epsilon}, \dots, \frac{\pi_\rho^s}{\epsilon^{\rho-1}}, \eta, \hat{z}_\rho, \hat{\alpha}_{\rho-1}]^T$ respectively, for $i = 2, \dots, \rho$. Therefore, the control laws are given by

$$\begin{aligned} \hat{\alpha}_1 &= -k_1 z_1 + \dot{y}_d, \\ \hat{\alpha}_i &= -k_i \hat{z}_i - \hat{z}_{i-1} + \hat{\alpha}_{i-1}, \end{aligned} \quad (4.58)$$

$$u_{nn} = \hat{W}^T S(\hat{V}^T \hat{Z}), \quad (4.59)$$

$$u_b = -k_\rho \hat{z}_\rho - \hat{z}_{\rho-1} - k_b \left(\left\| \hat{Z} \hat{W}^T \hat{S}'_o \right\|_F^2 + \left(\left\| \hat{S}_o \right\| + \left\| \hat{S}'_o \hat{V}^T \hat{Z} \right\| \right)^2 \right) \hat{z}_\rho \quad (4.60)$$

Due to the fact that the actual NN is in terms of \hat{Z} while the ideal NN is in terms of Z , the following Lemma is needed.

Lemma 4.17. [35] *The error between the actual and ideal NN output can be written as*

$$\hat{W}^T S(\hat{V}^T \hat{Z}) - W^{*T} S(V^{*T} Z) = \tilde{W}^T (\hat{S}_o - \hat{S}'_o \hat{V}^T \hat{Z}) + \hat{W}^T \hat{S}'_o \tilde{V}^T \hat{Z} + d_u \quad (4.61)$$

where $\hat{S}_o := S(\hat{V}^T \hat{Z})$; $\hat{S}'_o := \text{diag}\{\hat{s}'_{o1}, \dots, \hat{s}'_{ol}\}$ with

$$\hat{s}'_{oi} = s'(v_i^T \hat{Z}) = \left. \frac{ds(z_a)}{dz_a} \right|_{z_a = v_i^T \hat{Z}}, \quad i = 1, 2, \dots, l, \quad (4.62)$$

and the residual term d_u is bounded by

$$d_u \leq \|W^*\| \left(\|\hat{S}'_o \hat{V}^T \hat{Z}\| + \|\hat{S}_o\| \right) + \|V^*\|_F \|\hat{Z} \hat{W}^T \hat{S}'_o\|_F \quad (4.63)$$

Accordingly, the adaptation laws are designed as

$$\dot{\hat{W}} = -\Gamma_W \left[(\hat{S}_o - \hat{S}'_o \hat{V}^T \hat{Z}) \hat{z}_\rho + \sigma_W \hat{W} \right] \quad (4.64)$$

$$\dot{\hat{V}} = -\Gamma_V \left[\hat{Z} \hat{W}^T \hat{S}'_o \hat{z}_\rho + \sigma_V \hat{V} \right] \quad (4.65)$$

Using the backstepping procedure similar to Sect. 4.4.1, and substituting (4.59), (4.64), and (4.65) into the derivative of V_ρ along the closed loop trajectories, it can be shown that

$$\begin{aligned} \dot{V}_\rho \leq & -\sum_{j=1}^{\rho-1} k_j z_j^2 - \left(g_0 + \frac{\dot{g}\lambda}{2g\lambda} \right) \frac{z_\rho^2}{g\lambda} - \sum_{j=2}^{\rho-1} k_j z_j \tilde{z}_j + \sum_{j=2}^{\rho-1} z_j (\dot{\alpha}_{j-1} - \dot{\alpha}_{j-1}) \\ & + \sum_{j=3}^{\rho-1} z_j \tilde{z}_{j-1} - z_\rho \varepsilon - \tilde{W}^T \left[(\hat{S}_o - \hat{S}'_o \hat{V}^T \hat{Z}) \hat{z}_\rho + \sigma_W \hat{W} \right] \\ & - \text{tr} \left\{ \tilde{V}^T \left[\hat{Z} \hat{W}^T \hat{S}'_o \tilde{z}_\rho + \sigma_V \hat{V} \right] \right\} + |z_\rho| \left[\|W^*\| \left(\|\hat{S}'_o \hat{V}^T \hat{Z}\| + \|\hat{S}_o\| \right) \right. \\ & \left. + \|V^*\|_F \|\hat{Z} \hat{W}^T \hat{S}'_o\|_F \right] + z_\rho u_b \end{aligned} \quad (4.66)$$

From the inequalities in (4.33) and (4.34), we know that

$$\begin{aligned}
\dot{V}_\rho \leq & -\sum_{j=1}^{\rho-1} k_j z_j^2 - \left(g_0 + \frac{\dot{g}_\lambda}{2g_\lambda}\right) \frac{z_\rho^2}{g_\lambda} - \sum_{j=2}^{\rho-1} k_j z_j \tilde{z}_j + \sum_{j=2}^{\rho-1} z_j (\dot{\alpha}_{j-1} - \dot{\alpha}_{j-1}) \\
& + \sum_{j=3}^{\rho-1} z_j \tilde{z}_{j-1} - z_\rho \varepsilon - \tilde{W}^T (\hat{S}_o - \hat{S}'_o \hat{V}^T \hat{Z}) \tilde{z}_\rho - \hat{W}^T \hat{S}'_o \tilde{V}^T \hat{Z} \tilde{z}_\rho \\
& + \frac{\sigma_W}{2} (-\|\tilde{W}\|^2 + \|W^*\|^2) + \frac{\sigma_V}{2} (-\|\tilde{V}\|_F^2 + \|V^*\|_F^2) + \frac{1}{2} \|W^*\|^2 \\
& + \frac{1}{2} \|V^*\|_F^2 + \frac{1}{2} z_\rho^2 \left[\left(\|\hat{S}'_o \hat{V}^T \hat{Z}\| + \|\hat{S}_o\| \right)^2 + \|\hat{Z} \hat{W}^T \hat{S}'_o\|_F^2 \right] + z_\rho u_b
\end{aligned} \tag{4.67}$$

Substituting the bounding control (4.60) into (4.66) yields

$$\begin{aligned}
\dot{V}_\rho \leq & -\sum_{j=1}^{\rho-1} k_j z_j^2 - \left(k_\rho - \frac{1}{2}\right) z_\rho^2 - \left(g_0 + \frac{\dot{g}_\lambda}{2g_\lambda}\right) \frac{z_\rho^2}{g_\lambda} - \frac{\sigma_W}{2} \|\tilde{W}\|^2 - \frac{\sigma_V}{2} \|\tilde{V}\|_F^2 \\
& - \tilde{W}^T (\hat{S}_o - \hat{S}'_o \hat{V}^T \hat{Z}) \tilde{z}_\rho - \hat{W}^T \hat{S}'_o \tilde{V}^T \hat{Z} \tilde{z}_\rho - \sum_{j=2}^{\rho} k_j z_j \tilde{z}_j + \sum_{j=2}^{\rho} z_j (\dot{\alpha}_{j-1} \\
& - \dot{\alpha}_{j-1}) + \sum_{j=3}^{\rho} z_j \tilde{z}_{j-1} + \frac{\sigma_W + 1}{2} \|W^*\|^2 + \frac{\sigma_V + 1}{2} \|V^*\|_F^2 + \frac{1}{2} \varepsilon^2 \\
& - \left(k_b - \frac{1}{2}\right) \left[\left(\|\hat{S}'_o \hat{V}^T \hat{Z}\| + \|\hat{S}_o\| \right)^2 + \|\hat{Z} \hat{W}^T \hat{S}'_o\|_F^2 \right] (z_\rho^2 + z_\rho \tilde{z}_\rho)
\end{aligned} \tag{4.68}$$

The following lemma is useful for handling the terms containing the estimation errors \tilde{z}_j , for $j = 1, 2, \dots, \rho$.

Lemma 4.18. *There exist positive constants F_i and G_i , which are independent of ϵ , such that, for $t > t^*$, $i = 1, 2, \dots, \rho - 1$, the estimates $\hat{\alpha}_i$ and \hat{z}_i satisfy the following inequalities:*

$$|\dot{\hat{\alpha}}_i - \dot{\alpha}_i| \leq \epsilon F_i, \quad |\tilde{z}_i| := |\hat{z}_i - z_i| \leq \epsilon G_i. \tag{4.69}$$

Proof. Starting from $i = 1$, we know that

$$\dot{\hat{\alpha}}_1 - \dot{\alpha}_1 = -k_1(\hat{z}_1 - z_1) = -k_1\tilde{\xi}_2. \quad (4.70)$$

Subsequently, it is easy to obtain that

$$\begin{aligned} \dot{\hat{\alpha}}_2 - \dot{\alpha}_2 &= -k_2(\tilde{\xi}_3 - (\dot{\hat{\alpha}}_1 - \dot{\alpha}_1)) - \tilde{\xi}_2 - k_1\tilde{\xi}_3 \\ &= -(1 + k_1k_2)\tilde{\xi}_2 - (k_1 + k_2)\tilde{\xi}_3 =: a_2^T\Psi_2 \end{aligned} \quad (4.71)$$

where $a_2 := [-(1 + k_1k_2) \quad -(k_1 + k_2)]^T$ and $\Psi_2 := [\tilde{\xi}_2 \quad \tilde{\xi}_3]^T$. Suppose that

$$\begin{aligned} \dot{\hat{\alpha}}_{i-2} - \dot{\alpha}_{i-2} &= a_{i-2}^T\Psi_{i-2}, \\ \dot{\hat{\alpha}}_{i-1} - \dot{\alpha}_{i-1} &= a_{i-1}^T\Psi_{i-1}, \end{aligned} \quad (4.72)$$

where $\Psi_j = [\tilde{\xi}_2 \dots \tilde{\xi}_{j+1}]^T$ and a_j is a vector of constants, for $j = i-2, i-1$. Then, by induction, it can be shown that

$$\begin{aligned} \dot{\hat{\alpha}}_i - \dot{\alpha}_i &= -k_i \left(\tilde{\xi}_{i+1} - (\dot{\hat{\alpha}}_{i-1} - \dot{\alpha}_{i-1}) \right) - \left(\tilde{\xi}_i - (\dot{\hat{\alpha}}_{i-2} - \dot{\alpha}_{i-2}) \right) + \ddot{\alpha}_{i-1} - \ddot{\alpha}_{i-1}, \\ &= -k_i \left(\tilde{\xi}_{i+1} - a_{i-1}^T\Psi_{i-1} \right) - \left(\tilde{\xi}_i - a_{i-2}^T\Psi_{i-2} \right) + a_{i-1}^T\dot{\Psi}_{i-1} = a_i^T\Psi_i \end{aligned} \quad (4.73)$$

for $i = 3, \dots, \rho - 1$. From Lemma 4.15, we know that $\|\Psi_i\| \leq \epsilon H_i$, where $H_i := \|[h_2, \dots, h_{i+1}]^T\|$, which leads to the fact that $|\dot{\hat{\alpha}}_i - \dot{\alpha}_i| \leq \epsilon \|a_i\| H_i =: \epsilon F_i$, and thus (4.69) is proven.

To prove (4.69), note that

$$\begin{aligned} \tilde{z}_i &= \tilde{\xi}_i - (\hat{\alpha}_{i-1} - \alpha_{i-1}) \\ &= \tilde{\xi}_i - (-k_{i-1}\tilde{z}_{i-1} - \tilde{z}_{i-2} + \dot{\hat{\alpha}}_{i-1} - \dot{\alpha}_{i-1}) \end{aligned} \quad (4.74)$$

By following a similar inductive procedure, starting from $\tilde{z}_1 = \tilde{\xi}_1$ and $\tilde{z}_2 = \tilde{\xi}_2 - (\hat{\alpha}_1 - \alpha_1) = \tilde{\xi}_2$, it can be shown that $\tilde{z}_i = a_{zi}^T\Psi_i$, where a_{zi} is a constant vector. Using the property in (4.69), it is straightforward to see that $|\tilde{z}_i| \leq \epsilon \|a_{zi}\| H_i =: \epsilon G_i$. The proof is now complete. \square

Using Lemma 4.18, it is clear that, for $t > t^*$, the following inequalities hold:

$$-\tilde{W}^T(\hat{S}_o - \hat{S}'_o\hat{V}^T\hat{Z})\tilde{z}_\rho \leq \frac{\epsilon}{2}\|\tilde{W}\|^2 + \frac{\epsilon}{2}\left(\|\hat{S}_o\| + \|\hat{S}'_o\hat{V}^T\hat{Z}\|\right)^2 G_\rho^2, \quad (4.75)$$

$$-\hat{W}^T\hat{S}'_o\tilde{V}^T\hat{Z}\tilde{z}_\rho \leq \frac{\epsilon}{2}\|\tilde{V}\|_F^2 + \frac{\epsilon}{2}\left\|\hat{Z}\hat{W}^T\hat{S}'_o\right\|_F^2 G_\rho^2, \quad (4.76)$$

$$-\sum_{j=2}^{\rho} k_j z_j \tilde{z}_j \leq \sum_{j=2}^{\rho} \frac{k_j}{2} (z_j^2 + \epsilon^2 G_j^2), \quad (4.77)$$

$$\sum_{j=2}^{\rho-1} z_j (\dot{\alpha}_{j-1} - \dot{\alpha}_{j-1}) \leq \sum_{j=2}^{\rho} \frac{1}{2} (z_j^2 + \epsilon^2 F_j^2), \quad (4.78)$$

$$\sum_{j=3}^{\rho} z_j \tilde{z}_{j-1} \leq \sum_{j=3}^{\rho} \frac{1}{2} (z_j^2 + \epsilon^2 G_{j-1}^2). \quad (4.79)$$

By substitution of the inequalities (4.75)–(4.79) into (4.68), it is straightforward to obtain the following expression:

$$\begin{aligned} \dot{V}_\rho \leq & -\sum_{j=1}^{\rho-1} k_j z_j^2 - \left(k_\rho - \frac{1}{2}\right) z_\rho^2 - \left(g_0 + \frac{\dot{g}_\lambda}{2g_\lambda}\right) \frac{z_\rho^2}{g_\lambda} - \frac{(\sigma_W - \epsilon)}{2} \|\tilde{W}\|^2 \\ & - \frac{(\sigma_V - \epsilon)}{2} \|\tilde{V}\|_F^2 + \left[\left(\|\hat{S}_o\| + \|\hat{S}'_o \hat{V}^T \hat{Z}\|\right)^2 + \|\hat{Z} \hat{W}^T \hat{S}'_o\|_F^2 \right] \frac{\epsilon}{2} G_\rho^2 \\ & + \sum_{j=2}^{\rho} \frac{k_j}{2} (z_j^2 + \epsilon^2 G_j^2) + \sum_{j=2}^{\rho} \frac{1}{2} (z_j^2 + \epsilon^2 F_j^2) + \sum_{j=3}^{\rho} \frac{1}{2} (z_j^2 + \epsilon^2 G_{j-1}^2) \\ & + \frac{\sigma_W + 1}{2} \|W^*\|^2 + \frac{\sigma_V + 1}{2} \|V^*\|_F^2 + \frac{1}{2} \bar{\epsilon}^2 \\ & - \frac{1}{2} \left(k_b - \frac{1}{2}\right) \left[\left(\|\hat{S}'_o \hat{V}^T \hat{Z}\| + \|\hat{S}_o\|\right)^2 + \|\hat{Z} \hat{W}^T \hat{S}'_o\|_F^2 \right] (z_\rho^2 - \epsilon^2 G_\rho^2) \end{aligned} \quad (4.80)$$

The RHS terms can be rearranged into a more convenient form for analysis:

$$\begin{aligned} \dot{V}_\rho \leq & -k_1 z_1^2 - \frac{1}{2} (k_2 - 1) z_2^2 - \sum_{j=3}^{\rho-1} \frac{1}{2} (k_j - 2) z_j^2 - \frac{1}{2} (k_\rho - 3) z_\rho^2 - \left(g_0 + \frac{\dot{g}_\lambda}{2g_\lambda}\right) \frac{z_\rho^2}{g_\lambda} \\ & - \frac{(\sigma_W - \epsilon)}{2} \|\tilde{W}\|^2 - \frac{(\sigma_V - \epsilon)}{2} \|\tilde{V}\|_F^2 + \sum_{j=2}^{\rho} \frac{k_j}{2} \epsilon^2 G_j^2 + \sum_{j=2}^{\rho} \frac{1}{2} \epsilon^2 F_j^2 \\ & + \sum_{j=3}^{\rho} \frac{1}{2} \epsilon^2 G_{j-1}^2 + \frac{\sigma_W + 1}{2} \|W^*\|^2 + \frac{\sigma_V + 1}{2} \|V^*\|_F^2 + \frac{1}{2} \bar{\epsilon}^2 \\ & - \frac{1}{2} \left(k_b - \frac{1}{2}\right) \left[\left(\|\hat{S}'_o \hat{V}^T \hat{Z}\| + \|\hat{S}_o\|\right)^2 + \|\hat{Z} \hat{W}^T \hat{S}'_o\|_F^2 \right] (z_\rho^2 \\ & - \left(\epsilon^2 + \frac{2\epsilon}{2k_b - 1}\right) G_\rho^2). \end{aligned} \quad (4.81)$$

Finally, by appropriately choosing the control parameters k_ρ and k_b as follows:

$$k_2 > 1, \quad k_3, \dots, k_{\rho-1} > 2, \quad k_\rho > 3, \quad k_b > \frac{1}{2}, \quad \sigma_W, \sigma_V > \epsilon, \quad (4.82)$$

it can be shown that

$$\dot{V}_\rho \leq -c_1 V_\rho + c_2 - K \left(z_\rho^2 - \epsilon c_3 \right), \quad (4.83)$$

where

$$c_1 := \min \left\{ 2k_1, (k_2 - 1), (k_3 - 2), \dots, (k_{\rho-1} - 2), \underline{g}(k_\rho - 3), \frac{(\sigma_W - \epsilon)}{\lambda_{\max}(\Gamma_W^{-1})}, \frac{(\sigma_V - \epsilon)}{\lambda_{\max}(\Gamma_W^{-1})} \right\}, \quad (4.84)$$

$$c_2 := \frac{1}{2}\bar{\epsilon}^2 + \frac{\sigma_W + 1}{2} \|W^*\|^2 + \frac{\sigma_V + 1}{2} \|V^*\|_F^2 + \frac{1}{2}\epsilon^2 \left(\sum_{j=2}^{\rho} F_j^2 + \sum_{j=2}^{\rho-1} (k_j + 1)G_j^2 + G_\rho^2 \right), \quad (4.85)$$

$$c_3 := \left(\epsilon + \frac{2}{2k_b - 1} \right) G_\rho^2, \quad (4.86)$$

$$K := \frac{1}{2} \left(k_b - \frac{1}{2} \right) \left[\left(\|\hat{S}'_o \hat{V}^T \hat{Z}\| + \|\hat{S}_o\| \right)^2 + \|\hat{Z} \hat{W}^T \hat{S}'_o\|_F^2 \right]. \quad (4.87)$$

It can be shown that

$$\dot{V}_\rho(t) \leq -c_{o1} V_\rho(t) + c_{o2}, \quad t \geq t^* \\ c_{o1} := \min \left\{ 2\lambda_{\min}(K_1), \frac{\lambda_{\min}(K_2 - \frac{3}{2}I)}{\lambda_{\max}(M)}, \frac{\min_{i=1,2,3} \left\{ \frac{\sigma_i}{4} \|\tilde{\theta}_i\|^2 \right\}}{\lambda_{\max}(\Gamma^{-1})} \right\} \quad (4.88)$$

$$c_{o2} := \sum_{i=1}^3 \left(1 + \frac{\sigma_i}{2} \right) \|\theta_i^*\|^2 + \frac{1}{2} \|\epsilon\|^2 + 2\lambda_{\max}(\bar{K}_2 \bar{K}_2^T + \Lambda) \epsilon \kappa_2 \quad (4.89)$$

To ensure that $\rho > 0$, the control gains K_1 and K_2 are chosen to satisfy the following conditions:

$$\lambda_{\min}(K_1) > 0, \quad \lambda_{\min} \left(K_2 - \frac{3}{2}I \right) > 0. \quad (4.90)$$

We are ready to summarize our results for the output feedback case under the following theorem.

Theorem 4.19. *Consider the helicopter dynamics (4.1) under Assumptions 4.1–4.5, with output feedback control laws (4.59)–(4.60), adaptation laws (4.64)–(4.65), and high gain observer (4.53) which is turned on at time t^* in advance. For initial conditions $\xi(0)$, $\eta(0)$, $\tilde{W}(0)$, $\tilde{V}(0)$ starting in any compact set Ω_0 , all closed loop signals are SGUUB, and the tracking error z_1 converges to the steady state compact set:*

$$\Omega_{z_1} := \left\{ z_1 \in R \mid |z_1| \leq \sqrt{\frac{2\bar{c}_2}{c_1}} \right\}, \quad (4.91)$$

where $\bar{c}_2 := c_2 + c_3\bar{K}$, and c_1 is as defined in (4.84).

Proof. We consider the following two cases for the stability analysis:

Case 1: $|z_\rho| > \sqrt{\epsilon c_3}$

For this case, the last term of (4.83) is negative, thus yielding

$$\dot{V}_\rho \leq -c_1 V_\rho + c_2, \quad (4.92)$$

which straightforwardly implies that all closed loop signals are SGUUB, according to Lemma 4.9. However, when $|z_\rho| \leq \sqrt{\epsilon c_3}$, the last term of (4.83) may not be negative, leading to a more complicated analysis, as shown in the subsequent case.

Case 2: $|z_\rho| \leq \sqrt{\epsilon c_3}$

For this case, we want to show that, as a result of z_ρ being bounded, the function K in (4.87) is also bounded, for which (4.83) can be expressed in the form of (4.9), convenient for establishing SGUUB property. To this end, note that the derivative of $V_{\rho-1}$ is given by

$$\dot{V}_{\rho-1} \leq -\sum_{i=1}^{\rho-1} k_i z_i^2 - \sum_{i=2}^{\rho-1} k_i z_i \tilde{z}_i + \sum_{i=2}^{\rho-1} z_i (\dot{\hat{\alpha}}_{i-1} - \hat{\alpha}_{i-1}) + \sum_{i=3}^{\rho-1} z_i \tilde{z}_{i-1} + z_{\rho-1} z_\rho \quad (4.93)$$

According to Lemma 4.18, we can show that

$$\begin{aligned} \dot{V}_{\rho-1} &\leq -\sum_{i=1}^{\rho-1} k_i z_i^2 + \sum_{i=2}^{\rho-1} k_i |z_i| \epsilon G_i + \sum_{i=2}^{\rho-1} |z_i| \epsilon F_i + \sum_{i=3}^{\rho-1} |z_i| \epsilon G_{i-1} + |z_{\rho-1}| \sqrt{\epsilon c_3} \\ &\leq -k_1 z_1^2 - \frac{1}{2}(k_2 - 1)z_2^2 - \sum_{i=3}^{\rho-2} \frac{1}{2}(k_i - 2)z_i^2 - \frac{1}{2}(k_\rho - 3)z_{\rho-1}^2 \end{aligned}$$

$$\begin{aligned}
& + \frac{1}{2}\epsilon c_3 + \frac{1}{2} \sum_{i=3}^{\rho-1} \epsilon^2 G_{i-1}^2 + \frac{1}{2} \sum_{i=2}^{\rho-1} \epsilon^2 F_i^2 + \frac{1}{2} \sum_{i=2}^{\rho-1} k_i \epsilon^2 G_i^2 \\
& \leq -c_4 V_{\rho-1} + c_5,
\end{aligned} \tag{4.94}$$

where the positive constants c_4 and c_5 are defined by

$$c_4 := \min\{2k_1, k_2 - 1, k_3 - 2, \dots, k_{\rho-1} - 2, k_\rho - 3\}, \tag{4.95}$$

$$c_5 := \frac{\epsilon}{2} \left[c_3 + \epsilon \left(\sum_{i=2}^{\rho-1} F_i^2 + \sum_{i=2}^{\rho-2} (1 + k_i) G_i^2 + k_{\rho-1} G_{\rho-1}^2 \right) \right]. \tag{4.96}$$

This implies that $z(t)$ satisfies the inequality

$$\|z(t)\| \leq \sqrt{2 \left(V_{\rho-1}(0) + \frac{c_5}{c_4} \right) + \epsilon c_3} =: \bar{z}. \tag{4.97}$$

According to Lemma 4.11, it follows from the boundedness of $z(t)$ that the internal states $\eta(t)$ are also bounded, i.e.,

$$\|\eta(t)\| \leq a_1(\bar{z} + \bar{\xi}_d) + a_2 =: \bar{\eta}, \tag{4.98}$$

where $\|\xi_d(t)\| \leq \bar{\xi}_d$ for constant $\bar{\xi}_d > 0$, based on Assumption 4.1. Thus, the vector of NN inputs \hat{Z} is also bounded as follows

$$\|\hat{Z}\| \leq \left\| \left[\xi_{1d} + \bar{z}, \frac{\bar{\pi}_2}{\epsilon}, \dots, \frac{\bar{\pi}_\rho}{\epsilon^{\rho-1}}, \bar{\eta}, \sqrt{c_3} + \epsilon G_\rho, \bar{\alpha}_{\rho-1} + \epsilon F_{\rho-1} \right]^T \right\| =: \bar{Z} \tag{4.99}$$

where the constant $\bar{\alpha}_{\rho-1} > 0$ is an upper bound for $\alpha_{\rho-1}(z, \xi_{1d}, \xi_{1d}^{(1)}, \dots, \xi_{1d}^{(\rho)})$. Exploiting the properties of sigmoidal NNs [30], it can be shown that

$$\left(\|\hat{S}'_o \hat{V}^T \hat{Z}\| + \|\hat{S}_o\|_F \right) \leq 1.224 \sqrt{l}. \tag{4.100}$$

As a result, from the adaptation law (4.64), the dynamics of the neural weights $\hat{W} = [\hat{W}_1, \dots, \hat{W}_l, \dots, \hat{W}_l]^T$ can be shown to satisfy the inequality

$$\dot{\hat{W}} \leq -\lambda_{\min}(\Gamma_W) \sigma_W \hat{W} + 1.224 \sqrt{l} \lambda_{\min}(\Gamma_W) (\sqrt{\epsilon c_3} + \epsilon G_\rho), \tag{4.101}$$

which results in

$$\|\hat{W}(t)\| \leq \|\hat{W}(0)\| + \frac{1.224 \sqrt{l} (\sqrt{\epsilon c_3} + \epsilon G_\rho)}{\sigma_W} =: \bar{W}, \tag{4.102}$$

where \bar{W} is a positive constant. Accordingly, from (4.87), and the fact that $\|S'_o\|_F \leq 0.25\mu\sqrt{l}$, we can show that K is bounded as follows:

$$K \leq \frac{l}{2} \left(k_b - \frac{1}{2} \right) \left[1.498 + 0.0625 \left(\bar{Z} \bar{W} \mu \right)^2 \right] =: \bar{K}, \quad (4.103)$$

where \bar{K} is a positive constant. From (4.83) and (4.103), we obtain that

$$\dot{V}_\rho \leq -c_1 V_\rho + \bar{c}_2, \quad (4.104)$$

where $\bar{c}_2 := c_2 + \epsilon c_3 \bar{K}$ is a positive constant.

Having obtained (4.104) for Case 2, we can compare it with (4.92) of Case 1 to see that (4.104) describes a larger compact set in which the closed loop signals remain, by virtue of the fact that $\bar{c}_2 \geq c_2$. Hence, the performance bounds can be analyzed from (4.104), as a conservative approach. A nice property is that as ϵ diminishes to zero, we have $\bar{c}_2 \rightarrow c_2$, and the performance can be analyzed from (4.92) instead, albeit conservatively.

Based on (4.104), we can directly invoke Lemma 4.9 to conclude SGUUB for all closed loop signals. Since it is straightforward to prove that the tracking error $z_1 = \xi_1 - \xi_{1d}$ converges to the compact set Ω_{z_1} , by following the steps outlined in the proof of Theorem 4.12, we have omitted the proof. \square

Remark 4.20. It follows from Theorem 4.19 that the size of the steady state compact set Ω_{z_1} , to which the tracking error converges, depends on the ratio $\frac{\bar{c}_2}{c_1}$, which contain tunable parameters. Thus, we can reduce the size of Ω_{z_1} by appropriately choosing the parameters. For instance, by choosing the control gains k_1, \dots, k_ρ large and the observer parameter ϵ sufficiently small, the ratio $\frac{\bar{c}_2}{c_1}$ can be decreased, to the effect that Ω_{z_1} diminishes.

4.5 Simulation Study

In Sect. 4.2, we have considered a general representation of helicopters as nonaffine nonlinear systems. Although it would be more realistic to perform simulations on nonaffine helicopter models, an accurate model is difficult to obtain. Since the class of nonaffine systems include linear systems as special cases, we shall apply our proposed adaptive NN control for general nonlinear systems to linear and nonlinear affine helicopter models, which are available in the literature.

In particular, we will first investigate the effectiveness of the NN controller on a linear helicopter model for two tasks: altitude tracking and pitch tracking. For the altitude tracking task, we will compare our results with that of [54], while for the pitch tracking study, we will compare with [38]. This will be followed by a study for the case of a nonlinear helicopter model for vertical flight.

For all cases, we use a multi-layer NN as detailed in Sect. 4.3.2, with identical neuronal activation functions for the hidden layer described by

$$s_i(z_a) = \frac{1}{1 + e^{-\mu z_a}}, \quad i = 1, 2, \dots, l, \quad (4.105)$$

so that $S(a) = [s_1(a_1), s_2(a_2), \dots, s_l(a_l)]^T$. The control law is given by (4.24) and the adaptation laws by (4.30)–(4.31).

4.5.1 Linear Models

In this section, we consider two linearized helicopter models for altitude and pitch tracking. Since data on linear models is quite rich in the literature, it is useful to employ them in a study of the effectiveness of the proposed nonlinear NN controller. As linear systems are a special subclass of nonlinear nonaffine systems, the NN controller, which is designed for the latter, can be applied on linear systems without any complications.

4.5.1.1 Altitude Tracking

To this end, consider the linearized altitude model of the Yamaha R50 helicopter as detailed in [54] with the longitudinal cyclic input δ set to zero:

$$\begin{bmatrix} \dot{u} \\ \dot{q} \\ \dot{\theta} \\ \dot{\beta} \\ \dot{\omega} \\ \dot{h} \end{bmatrix} = \begin{bmatrix} X_u & X_q & X_\theta & X_\beta & X_\omega & 0 \\ M_u & M_q & 0 & M_\beta & M_\omega & 0 \\ 0 & 1 & 0 & 0 & 0 & 0 \\ B_u & -1 & 0 & B_\beta & 0 & 0 \\ Z_u & Z_q & Z_\theta & Z_\beta & Z_\omega & 0 \\ 0 & 0 & 0 & 0 & -1 & 0 \end{bmatrix} \begin{bmatrix} u \\ q \\ \theta \\ \beta \\ \omega \\ h \end{bmatrix} + \begin{bmatrix} 0 \\ 0 \\ 0 \\ 0 \\ Z_\Omega \\ 0 \end{bmatrix} \delta_\Omega, \quad (4.106)$$

The control parameters are set to be $k_1 = 2.0$, $k_2 = 8.5$, and $k_b = 1.0$, while the NN parameters are $\mu = 1$, $\Gamma_W = 5I$, $\Gamma_V = 50I$, and $\sigma_W = \sigma_V = 5$. For the high gain observer, we choose $\epsilon = 0.01$, $\gamma_1 = 2$, and $\bar{\pi}_2 = 0.08$. The lower and upper saturation limits of the control are 393 rpm and 1,348 rpm respectively. The initial conditions are $x(0) = [10, 0, 0, 0, 0, 0]^T$, $\hat{W} = 0$, and $\hat{V} = 0$.

To compare our controller with that of [54], we consider the tracking of the altitude h according to a desired trajectory $h_d(t)$ defined by

$$\begin{bmatrix} \dot{h}_d \\ \ddot{h}_d \end{bmatrix} = \begin{bmatrix} 0 & 1 \\ -2.25 & -2.4 \end{bmatrix} \begin{bmatrix} h_d \\ \dot{h}_d \end{bmatrix} + \begin{bmatrix} 0 \\ 2.25 \end{bmatrix} h_{\text{ref}},$$

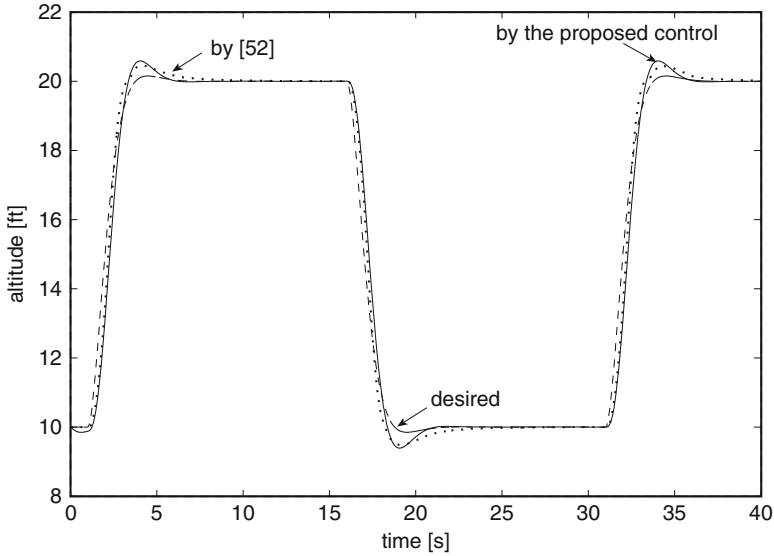


Fig. 4.1 Comparison of altitude tracking performance between the proposed controller and that of [54]

$$h_{\text{ref}}(t) = \begin{cases} 0 & \text{if } 0 \leq t < 1 \\ 10 & \text{if } 1 \leq t < 16 \\ 0 & \text{if } 16 \leq t < 31 \\ 10 & \text{if } t \geq 31 \end{cases} \quad (4.107)$$

Note that in our comparison, both controllers are simulated without engine dynamics.

It can be seen in Fig. 4.1 that the tracking performance under the proposed control is reasonably good, with the altitude signal tracking the desired trajectory closely. The comparison shows that the performances under the two different controls are similar. From Fig. 4.2, it is clear that the control signals and neural weights are well-behaved. The control of [54] exhibits more fluctuations, and the neural weights evolve to significantly larger amplitudes. Although this does not set out any comparative advantages, it does demonstrate different mechanisms at work in the two control schemes.

The effect of the parameter ϵ on tracking errors and observer errors are shown in Fig. 4.3, where it is seen that as ϵ diminishes, the tracking error under the full-state feedback control is recovered, and faster convergence of the observer is achieved.

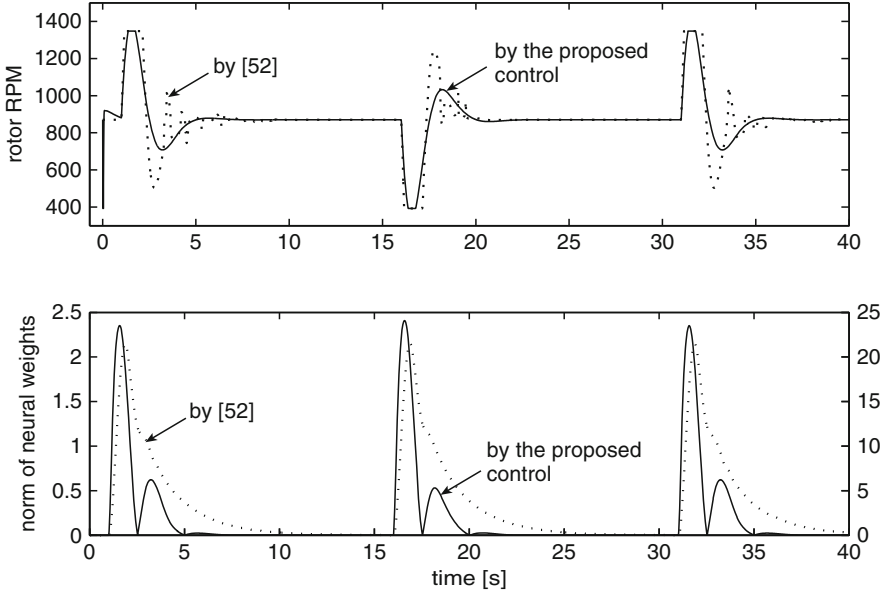


Fig. 4.2 Comparison of rotor RPM input and norm of neural weights, given by $\sqrt{\|\hat{W}^T\|^2 + \|\hat{V}\|_F^2}$, between the proposed control and that of [54]. For the bottom graph, the left scale corresponds to the proposed control while the right scale corresponds to that of [54]

4.5.1.2 Pitch Tracking

To this end, consider the linearized model of the Yamaha R50 helicopter with actuator dynamics as detailed in [38].

The control parameters are set to be $k_1 = 0.8, k_2 = 0.8, k_3 = 1.5$ and $k_b = 1.0$, while the NN parameters are $\mu = 0.01, \Gamma_W = 5I, \Gamma_V = 50I, \sigma_W = 5$, and $\sigma_V = 1$. For the high gain observer, we choose $\epsilon = 1 \times 10^{-4}, \gamma_1 = 3, \gamma_2 = 3, \bar{\pi}_2 = 4 \times 10^{-5}$, and $\bar{\pi}_3 = 4 \times 10^{-8}$. The initial conditions are $x(0) = 0, \hat{W} = 0$, and $\hat{V} = 0$.

Remark 4.21. Although it is stated in (4.82) that $k_2 > 1$ and $k_3 > 3$, those conditions obtained from theoretical analysis are somewhat conservative for this example, although they guarantee a stable, working controller. We found that the lower control gains chosen here are sufficiently good for obtaining satisfactory tracking performance.

To compare our controller with that of [38], we consider the tracking of the pitch angle θ according to a desired trajectory $\theta_d(t)$ defined by

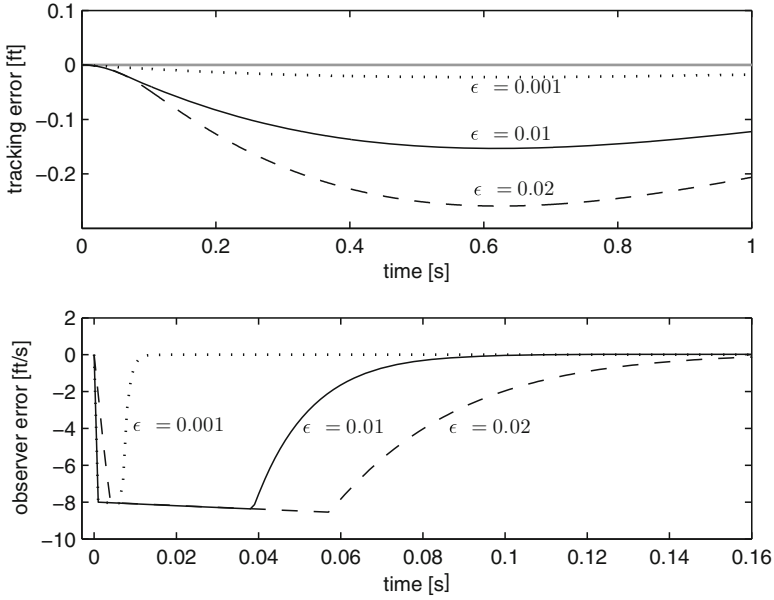


Fig. 4.3 Effect of ϵ on tracking errors and observer errors

$$\begin{bmatrix} \dot{\theta}_d \\ \ddot{\theta}_d \\ \dddot{\theta}_d \end{bmatrix} = \begin{bmatrix} 0 & 1 & 0 \\ 0 & 0 & 1 \\ -2,000 & -420 & -36 \end{bmatrix} \begin{bmatrix} \theta_d \\ \dot{\theta}_d \\ \ddot{\theta}_d \end{bmatrix} + \begin{bmatrix} 0 \\ 0 \\ 2,000 \end{bmatrix} \theta_{\text{ref}},$$

$$\theta_{\text{ref}}(t) = \begin{cases} 0 & \text{if } 0 \leq t < 0.5 \\ 0.1 & \text{if } 0.5 \leq t < 2 \\ 0 & \text{if } 2 \leq t < 3 \\ -0.1 & \text{if } 3 \leq t < 4.5 \\ 0 & \text{if } t \geq 4.5 \end{cases} . \quad (4.108)$$

It can be seen in Fig.4.4 that the tracking performance of our controller is comparable with that of [38] for the pitch tracking task. From Fig.4.5, we see that the control input and neural weights are bounded. Similar to the results in Sect.4.5.1.1, the control of [38] exhibits more fluctuations, and the neural weights are larger, illustrating the different mechanisms at work in the two control schemes.

4.5.2 Nonlinear Model

The previous section considered linearized models which are relatively easy to control, but tend to be more suited for local operation within a neighborhood

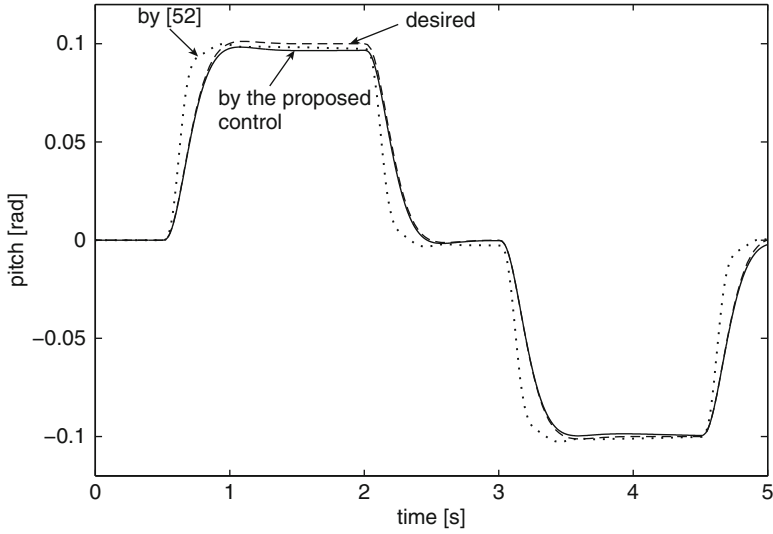


Fig. 4.4 Comparison of pitch tracking performance between the proposed control and that of [38]

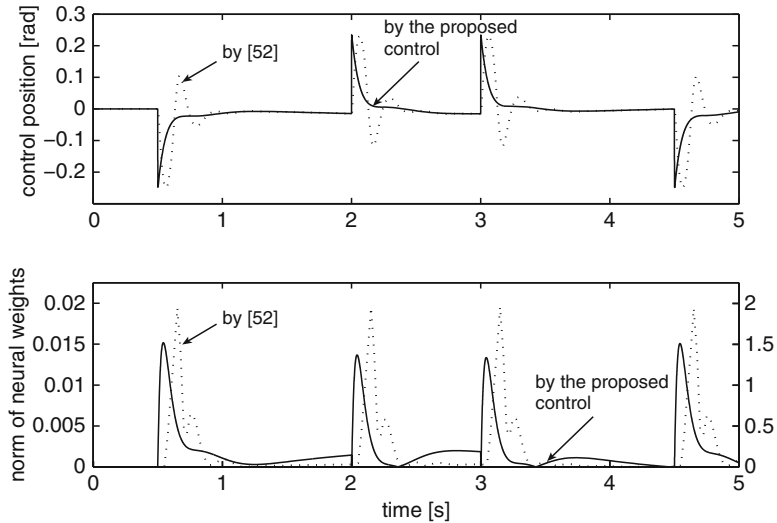


Fig. 4.5 Comparison of control input and norm of neural weights, given by $\sqrt{\|\hat{W}^T\|^2 + \|\hat{V}\|^2}$, between the proposed control and that of [38]. For the bottom graph, the *left scale* corresponds to the proposed control while the *right scale* corresponds to that of [38]

of the operating point, for which the linearized model is valid. Nevertheless, it was demonstrated that the proposed adaptive NN control is effective for the linear models considered, which constitute a subclass of general non-affine systems considered in the control design. In this section, we extend the investigations further

to the case of a nonlinear helicopter model. Both full-state and output feedback cases are considered.

Consider the nonlinear model of the X-cell 50 model helicopter in vertical flight [48, 93]:

$$\begin{aligned}
 \dot{x}_1 &= x_2 \\
 \dot{x}_2 &= a_0 + a_1 x_2 + a_2 x_2^2 + (a_3 + a_4 x_4 - \sqrt{a_5 + a_6 x_4}) x_3^2 \\
 \dot{x}_3 &= a_7 + a_8 x_3 + (a_9 \sin x_4 + a_{10}) x_3^2 + a_{th} \\
 \dot{x}_4 &= x_5 \\
 \dot{x}_5 &= a_{11} + a_{12} x_4 + a_{13} x_3^2 \sin x_4 + a_{14} x_5 - K_2 u \\
 y &= x_1,
 \end{aligned} \tag{4.109}$$

where x_1 denotes altitude; x_2 denotes altitude rate; x_3 denotes rotor speed; x_4 denotes the collective pitch angle; x_5 denotes the collective pitch rate; $a_{th} = 111.69 \text{s}^{-2}$ is a constant input to the throttle; and u is the input to the collective servomechanisms. The parameters are

$$\begin{aligned}
 K_1 &= -0.1088 \text{s}^{-2} & K_2 &= 0.25397 \text{s}^{-2} & a_0 &= -17.67 \text{ms}^{-2} \\
 a_1 &= -0.1 \text{s}^{-2} & a_2 &= -0.1 \text{s}^{-2} & a_3 &= 5.31 \times 10^{-4} \\
 a_4 &= 1.5364 \times 10^{-2} & a_5 &= 2.82 \times 10^{-7} & a_6 &= 1.632 \times 10^{-5} \\
 a_7 &= -13.92 \text{s}^{-2} & a_8 &= -0.7 \text{s}^{-2} & a_9 &= -0.0028 \\
 a_{10} &= -0.0028 & a_{11} &= 434.88 \text{s}^{-2} & a_{12} &= 800 \text{s}^{-2} \\
 a_{13} &= -0.1 & a_{14} &= -65 \text{s}^{-2}.
 \end{aligned} \tag{4.110}$$

Let output y be the altitude x_1 . By restricting the throttle input to be constant, we obtain a SISO system in which u is the only input variable forcing the output y to track a desired trajectory $y_d(t)$, which we define as

$$y_d(t) = 5.5 - 0.5 \sin t. \tag{4.111}$$

It can be shown that the system has strong relative degree 4, with the ξ subsystem given by

$$\begin{aligned}
 \dot{\xi}_1 &= \xi_2 = x_2 \\
 \dot{\xi}_2 &= \xi_3 = a_0 + a_1 x_2 + a_2 x_2^2 + (a_3 + a_4 x_4 - \sqrt{a_5 + a_6 x_4}) x_3^2 \\
 \dot{\xi}_3 &= \xi_4 = (a_1 + 2a_2 \xi_2) \xi_3 + a_3 x_3^2 + \left(a_4 - \frac{a_6}{2\sqrt{a_5 + a_6 x_4}} \right) x_3^2 x_5 \\
 &\quad + 2(a_3 + a_4 x_4 - \sqrt{a_5 + a_6 x_4}) x_3 (a_8 x_3 + (a_9 \sin x_4 + a_{10}) x_3^2) \\
 \dot{\xi}_4 &= b(x) + g(x) u_2,
 \end{aligned} \tag{4.112}$$

where

$$g(x) = -K_2 x_3^2 \left(a_4 - \frac{a_6}{2\sqrt{a_5 + a_6 x_4}} \right). \quad (4.113)$$

The derivation of $b(x)$ in (4.112) is omitted, and we proceed to verify that the system indeed satisfies the assumptions supposed in the control design. Assumptions 4.1 and 4.2 are obviously satisfied from (4.108) and (4.112) respectively.

To verify Assumption 4.4, we first note, from a practical standpoint, that the collective pitch angle, x_4 , is restricted within a range, typically from 0 to 0.44 rad [83]. It can be verified that the bracketed terms in (4.113) are virtually constant: they take values in the range $[1.4, 1.5] \times 10^{-3}$. Thus, the control coefficient $g(x)$ in (4.113) is always negative. Together with the fact that rotor speed x_3 is nonzero during flight, it can be concluded that there does not exist any control singularities or zero crossings of $g(x)$. Therefore, the first part of Assumption 4.4 is satisfied.

Remark 4.22. Although the second part of the assumption, that $g(x) > 0$, does not correspond to this example, there is no loss of applicability of the theoretical results, as explained in Remark 4.14. The control is still valid under a simple change of sign, i.e., $u = -u_{nn} - u_b$.

Lastly, it is not difficult to verify the existence of a function

$$g_0(x) = 2 \left(|a_8| + |a_9 \sin x_4 + a_{10}| |x_3| + \frac{\frac{a_6}{4(a_5 + a_6 x_4)^{1.5}}}{2 \left(a_4 - \frac{a_6}{2\sqrt{a_5 + a_6 x_4}} \right)} \right) > 0, \quad (4.114)$$

$$\forall x_3 \in R^+, \quad x_4 \in [0, 0.44],$$

which fulfils Assumption 4.5 for the case of $g(x) < 0$. Note that this function need not be known; we only need to show its existence.

The control parameters are chosen as $k_1 = 2.0$, $k_2 = 3.0$, $k_3 = 4.5$, $k_4 = 5.5$, $k_b = 0.6$, while the NN parameters are $\mu = 0.01$, $\Gamma_W = 50I$, $\Gamma_V = 20.4I$, $\sigma_V = 0.055$ and $\sigma_W = 0.05$. For the high gain observer, we choose $\epsilon = 5 \times 10^{-4}$, $\gamma_1 = 4$, $\gamma_2 = 6$, $\gamma_3 = 4$, $\bar{\pi}_2 = 5 \times 10^{-4}$, $\bar{\pi}_3 = 5 \times 10^{-8}$, and $\bar{\pi}_4 = 1 \times 10^{-11}$. The saturation limits of the control are ± 400 mrad. The initial conditions are $x(0) = [5.2, 0, 95.36, 0, 0]^T$, $\hat{W} = 0$, and $\hat{V} = 0$.

From Fig. 4.6, it can be seen that good tracking performance is achieved by the proposed adaptive NN control. The tracking performance for the full-state and output feedback cases are similar for the choice of ϵ made. The initial error is efficiently reduced and the altitude trajectory lies in close proximity of the desired sinusoidal trajectory. We compare the performance of the NN controller with a linear PD controller

$$u_{pd} = K_p(y - y_d) + K_d(\dot{y} - \dot{y}_d), \quad (4.115)$$

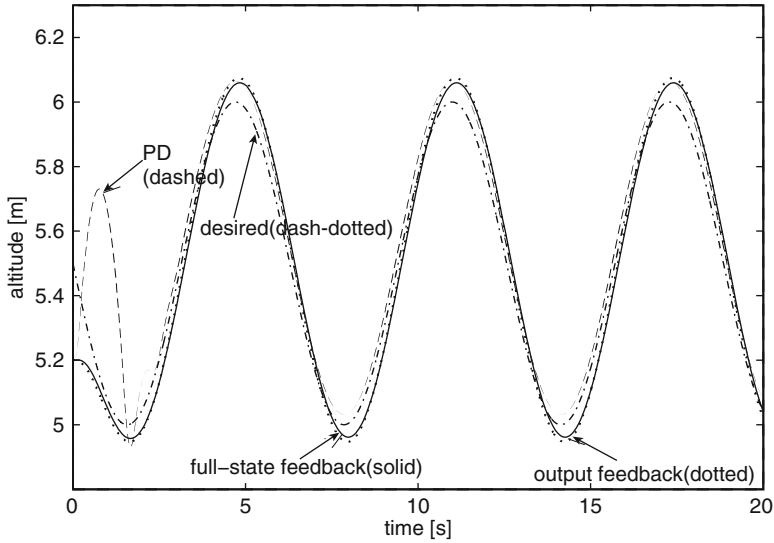


Fig. 4.6 Comparison of tracking performance between adaptive NN and PD control for nonlinear helicopter model

where $K_p = 5,000$ rad and $K_d = 500$ rad s are chosen so that the tracking errors are reasonably small and the control magnitude is constrained to $|u_{pd}| \leq 400$ mrad. Although steady state errors are comparable between PD and NN control, the PD control gives poorer transient performance as it attempts to compensate for the initial error, due to the inability of the linear PD control to adequately compensate for the effects of nonlinearity and coupling. Clearly, a dynamic model compensator is essential to achieve better performance.

The boundedness of the control input and the neural weights, for full-state and output feedback NN control, as well as the PD control, are shown in Fig. 4.7. The size of input signal under PD control is much larger than that under NN control, as seen by the fact that the PD control signal initially fluctuates between the saturation limits. This can be explained by the fact that a large PD control gain is required to compensate for nonlinearities, thus amplifying the control effort greatly when the initial error is large.

In Fig. 4.8, it is shown that the rotor speed and collective pitch angle, for both full-state and output feedback NN control, are bounded. In particular, it is confirmed that the collective pitch angle remains in the region $[0, 0.44]$ rad as restricted in practical operations.

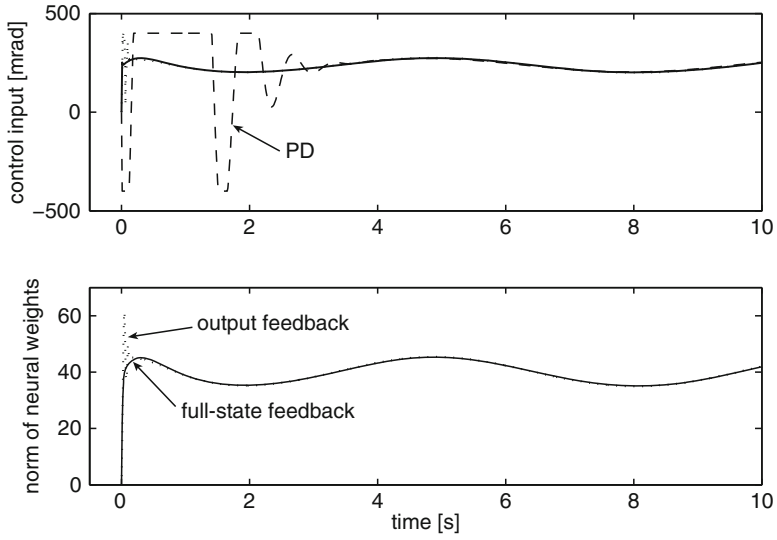


Fig. 4.7 *Top*: Control signals under adaptive NN and PD control. *Bottom*: Norm of neural weights, given by $\sqrt{\|\hat{W}^T\|^2 + \|\hat{V}\|_F^2}$, under full-state and output feedback NN control

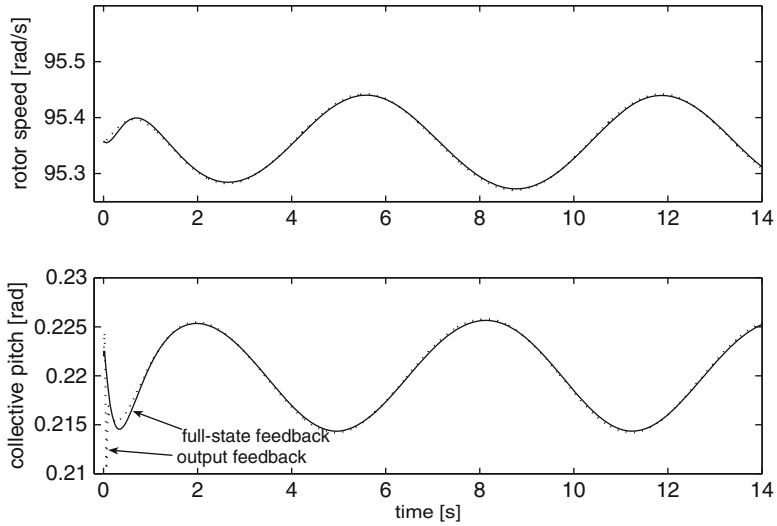


Fig. 4.8 *Top*: Speed of rotor. *Bottom*: Collective pitch angle

4.6 Conclusion

In this chapter, a robust adaptive NN control has been presented for helicopter systems whose dynamics are represented by a general nonlinear nonaffine form. Based on the use of the Implicit Function Theorem and the Mean Value Theorem, we proposed a constructive approach for stable adaptive NN control design with guaranteed performance bounds. We focused on SISO helicopter systems, which are valid for certain single-channel modes of operation, such as vertical flight and pitch regulation, and also for special conditions under which the multiple channels become decoupled. Considering both full-state and output feedback cases, it has been shown that, under the proposed NN control, the output tracking error converges to a small neighborhood of the origin, while the remaining closed-loop signals remain bounded. The extensive simulation study demonstrated the effectiveness of the proposed control on dynamic models of helicopters.